



Published in final edited form as:

Skeletal Radiol. 2013 November ; 42(11): 1583–1592. doi:10.1007/s00256-013-1703-7.

Characterization of soft tissue masses: can quantitative diffusion weighted imaging reliably distinguish cysts from solid masses?

Ty K. Subhawong,

Department of Radiology, University of Miami Miller School of Medicine, Jackson Memorial Hospital, 1611 NW 12th Ave, JMH WW 279, Miami, FL 33136, USA

Daniel J. Durand,

The Russell H. Morgan Department of Radiology and Radiological Science, The Johns Hopkins Hospital, 601 N. Wolfe St., Baltimore, MD 21287, USA

Gaurav K. Thawait,

The Russell H. Morgan Department of Radiology and Radiological Science, The Johns Hopkins Hospital, 601 N. Wolfe St., Baltimore, MD 21287, USA

Michael A. Jacobs,

The Russell H. Morgan Department of Radiology and Radiological Science, The Johns Hopkins Hospital, 601 N. Wolfe St., Baltimore, MD 21287, USA

Laura M. Fayad

The Russell H. Morgan Department of Radiology and Radiological Science, The Johns Hopkins Hospital, 601 N. Wolfe St., Baltimore, MD 21287, USA

Abstract

Objective—To investigate the accuracy of quantitative diffusion-weighted imaging (DWI) with apparent diffusion coefficient (ADC) mapping for characterizing soft tissue masses (STMs) as cysts or solid masses.

Materials and methods—This IRB-approved retrospective study included 36 subjects with 37 STMs imaged by conventional MRI (T1-weighted, T2-weighted, contrast-enhanced T1-weighted sequences) and DWI (b-values 50, 400, 800 s/mm²) with ADC mapping. STMs were defined as non-solid cysts by histology or clinical follow-up, and as solid by histology. For each STM, ADC values (range, mean) were recorded by two observers. Differences between ADC values in cysts and solid STMs were compared using Wilcoxon rank-sum and receiver-operating characteristic (ROC) analysis.

Results—There were higher minimum (1.65 vs 0.68, $p=0.003$) and mean (2.31 vs 1.45, $p=0.005$) ADC values in cysts than solid STMs respectively. Areas under the ROC for minimum and mean ADC values were 0.82 and 0.81 respectively. Using threshold ADC values of 1.8 (minimum) or 2.5 (mean) yielded a sensitivity of 60 % and 80 % respectively, and a specificity

of 100 % for classifying a STM as a cyst; for tumors with high fluid–signal intensity, the performance of these threshold values was maintained.

Conclusion—Diffusion-weighted imaging with ADC mapping provides a non-contrast MRI alternative for the characterization of STMs as cysts or solid masses. Threshold ADC values exist that provide 100 % specificity for differentiating cysts and solid STMs, even for tumors of high fluid–signal intensity on T2-weighted images.

Keywords

Diffusion-weighted imaging; Soft tissue tumors; ADC; T2-weighted; Musculoskeletal

Introduction

Magnetic resonance imaging (MRI) plays a critical role in the characterization of musculoskeletal soft tissue masses (STMs) [1], particularly in defining the size and extent of the lesion, and in delineating the involvement of adjacent viscera and the neurovascular structures. While simple lipomas and some fibrous tumors (such as quiescent fibromatosis) show characteristic MRI findings, definitive characterization of STMs using MRI alone is often not possible. In particular, some soft tissue neoplasms demonstrate T2 hyperintensity that can mimic cysts on unenhanced sequences [2]; misinterpretation of such lesions as cysts can lead to inappropriate surgical management [3]. As such, intravenous contrast medium is often administered for the assessment of STMs, first with the important purpose of differentiating solid tumors from cysts, and second, for further characterizing the enhancement patterns of solid soft tissue tumors. However, contrast medium administration requires intravenous access, may be precluded by renal failure, and adds a small, but non-negligible cost to the MR examination.

Diffusion-weighted imaging (DWI) is an unenhanced functional MRI technique based on perturbations to the Brownian motion of water caused by tissue microstructure and/or pathology. The apparent diffusion coefficient (ADC) is a quantitative measure of Brownian movement; highly cellular microenvironments in which diffusion is limited by the presence of cell membranes result in low ADC values, whereas acellular regions allowing for free diffusion in all directions are characterized by high ADC values [4]. In the musculoskeletal system, DWI has been used for the purpose of detection and the evaluation of treatment response in sarcoma patients undergoing chemotherapy [5–7]. For primary diagnosis, prior studies have shown mixed results regarding the ability of DWI to distinguish between benign and malignant STMs [8–11], although acellular cysts and myxoid tumors have been shown to have higher ADC values than other non-myxoid cellular tumors [9, 10, 12], for example, mean ADC of $1.92 \times 10^{-3} \text{ mm}^2/\text{s}$ in myxoid-containing tumors vs $0.97 \times 10^{-3} \text{ mm}^2/\text{s}$ in non-myxoid tumors [9]. We hypothesized that acellular cysts could therefore be distinguished from solid, cellular masses by their high ADC values. The main purpose of this study was to investigate the accuracy of quantitative DWI with ADC mapping for characterizing STMs as cysts or solid masses, and in particular, for distinguishing cysts from solid masses with high fluid content (such as myxoid tumors and synovial sarcoma). A secondary purpose of this study was to explore the accuracy of quantitative DWI for differentiating benign and malignant solid STMs. If proven accurate, quantitative DWI could provide an important

addition to a standard protocol for characterizing STMs, and potentially, a useful adjunct or alternative to contrast-enhanced imaging.

Materials and methods

Overview

In this IRB-approved retrospective study, the imaging of 36 subjects with 37 STMs who had undergone conventional MRI with T1-weighted, T2-weighted, and contrast-enhanced T1-weighted sequences as well as quantitative DWI with ADC mapping was reviewed. The ADC values of the STMs and the adjacent tissues were recorded. ADC measurements of non-solid STMs (defined by lack of enhancement or thin linear rim enhancement) and solid STMs (defined as contrast-enhancing lesions) were compared, as were benign and malignant solid STMs. Additionally, we performed a separate analysis focused on a sub-population of solid STMs with high fluid signal, to determine if the ADC values could differentiate true cysts from cystic-appearing solid STMs.

Subject population

Subjects who had undergone MRI with a tumor protocol for STM evaluation from April 2011 to July 2012 were identified through a picture archiving and communications system (PACS). 226 MRI studies were performed on STMs during the study period. One observer reviewed the radiology reports and selected subjects with STMs that were prospectively described as a “non-solid” STM (defined as a lesion without internal contrast enhancement) or “solid” STM (defined as any STM with reported internal enhancement following contrast medium administration). Then, patient demographic data and information on clinical follow-up from the clinical notes, as well as histological diagnoses from the pathology reports were recorded for each STM.

Inclusion criteria were subjects who had an STM that was referred for de novo evaluation prior to any treatment, a STM that was greater to or equal to 1 cm (in order to ensure an accurate measurement of the ADC values with a region of interest [ROI]) and subjects who had undergone MRI with a uniform DWI protocol (acquired with three b-values of 50, 400, and 800 mm²/s). Non-solid STMs were included if they had a histological diagnosis or if they met contrast-enhancement criteria (no internal enhancement) and had at least 3 months’ clinical follow-up indicating stability or resolution. Solid STMs were included only if they had a histological diagnosis. Exclusion criteria were lesions that were less than 1 cm (too small in which to accurately place an ROI), lesions that had already been treated with chemotherapy or radiation therapy, solid STMs without a histological diagnosis, solid lesions for which a definitive diagnosis could be made without contrast medium administration (e.g., lipoma), and lesions that were imaged without a complete DWI examination.

Of the original 226 MRI studies, 189 cases did not meet the inclusion criteria, (primarily because of a lack of diffusion-weighted imaging). The final subject population included 36 patients with 37 lesions (mean age 47.6 years, age range 4.4 to 87.1 years), and consisted of 20 male and 16 female patients. There were 10 lesions that were deemed “cysts.”

These included 6 simple cysts (ganglia, periarticular cysts) and 4 benign non-neoplastic non-solid lesions (lymphatic malformation, hematoma, seroma, and abscess). The remaining 27 lesions were deemed “solid” and included 15 benign STMs (8 peripheral nerve sheath tumors, 1 desmoid, 1 ganglioneuroma, 1 pigmented villonodular synovitis, 1 fibroblastic proliferation, 1 fibrosis, 1 exuberant inflammation, 1 inflammatory fibrovascular tissue) and 12 malignant soft tissue tumors (5 malignant peripheral nerve sheath tumors, 3 metastases, 1 myxoid sarcoma, 1 fibrosarcoma, 1 pleomorphic sarcoma, and 1 extraosseous Ewing’s sarcoma). For cysts, the diagnosis was established histologically ($n=3$) and/or by characteristic unenhancement on post-contrast imaging ($n=7$). For all solid STMs, the diagnosis was established histologically, either by percutaneous biopsy or final histology following surgical excision.

MRI protocol

All examinations were performed at 3 T (Trio or Verio; Siemens Medical Systems, Malvern, PA, USA). Anatomical imaging included T1-weighted (TR/TE 960/9, SL 5–6 mm) and fat-suppressed T2-weighted sequences (TR/TE 3,600–4,280/70, SL 5–6 mm) in the axial and coronal planes. After conventional anatomical imaging, but before intravenous contrast medium injection, DWI was performed in the axial plane using a spin-echo, single-shot echo-planar imaging (EPI) sequence. An inversion-recovery pulse (inversion time [TI]=180 ms) was implemented to exclude severe chemical-shift artifacts. The following parameters were used for DWI: TR=760 ms, TE=80 ms, NEX=2, gradient strength=25 mT/m, FOV=180–250 mm², matrix size=256×256 pixels, section thickness=5 mm, interslice gap=1 mm, section levels=30; a partial Fourier transform and EPI factor=88 was used; the b-values used were 50, 400, and 800 s/mm². These imaging parameters resulted in an imaging time of 2 min 32 s. ADC maps were calculated using a monoexponential fit with inline software from Siemens (Syngo MapIT). Then, a 3-D fat-suppressed T1-weighted sequence (volume interpolated breath-hold examination (VIBE), TR/TE 4.6/1.4, flip angle 9.5, SL 1 mm) was obtained prior to and following the administration of 0.1 mmol/kg body weight of gadolinium-diethylenetriamine pentaacetic acid (DTPA) (Magnevist; BayerSchering, Berlin, Germany). Subtraction imaging was applied to the contrast-enhanced sequences, with subtraction of the pre-contrast from post-contrast images.

Image analysis for conventional MRI

Two readers (one musculoskeletal radiology fellow and one musculoskeletal radiologist with 10 years’ experience), who were blinded to the histological diagnosis, retrospectively reviewed the conventional T1-weighted, T2-weighted, and contrast-enhanced T1-weighted sequences and recorded by consensus whether each STM was a cyst or solid STM according to the contrast-enhancement pattern. Cysts were defined as lesions with only thin linear rim enhancement and absence of internal enhancement. Solid STMs were defined as any lesion containing internal contrast enhancement (homogeneous or heterogeneous, including lesions with thick nodular peripheral enhancement, as may be seen with a centrally necrotic tumor).

Image analysis for quantitative T2 measurements

Because a focus of this study was T2 hyperintense STMs that simulate cysts, we quantified the T2 signal hyperintensity as a ratio of lesion:muscle signal simply as a way to identify

those lesions most likely to mimic true cysts owing to fluid-like signal. Such a ratio has been previously used to characterize soft tissue hemangiomas [13]. Each reader obtained quantitative measurements (performed at least 1 month apart) on the T2-weighted images by constructing a region of interest (ROI) to encompass as much of each mass as possible on a representative slice. The ROI size included at least 90 % of the mass and excluded adjacent tissues. Signal intensity was recorded within the mass, as well as within adjacent skeletal muscle (on the same slice) using a muscle ROI matching the size of the lesion ROI up to a maximum of 3 cm in diameter. A T2 signal ratio was defined as the ratio of the intensity of the STM to the intensity of skeletal muscle. Values across slices were averaged.

A subset of nine solid STMs with T2 hyperintensity approaching that of cysts was selected for sub-analysis, as these lesions with signal intensity similar to fluid are the most challenging to differentiate from true cysts. Similar measurements of T2 ratios (lesion:muscle or lesion:background ratios) have been reported in other organ systems, such as for pelvic cysts [14, 15], liver cysts [16], breast masses [17, 18], and brain lesions [19].

Image analysis for DWI

For each mass, diffusion-weighted images were reviewed in consensus and a qualitative assessment of the signal loss on successively higher b values was recorded on a four-grade scale (0, no signal loss; 1, mild signal loss; 2, moderate signal loss; 3, marked signal loss) [19].

Second, each reader constructed an ROI within each mass on the ADC map on up to three slices; if the mass was not large enough, ROIs were constructed on one ($n=5$) or two ($n=4$) slices. A ROI was also placed in the adjacent skeletal muscle on the same slice. Readers performed these measurements independently, at least 1 month apart. Minimum, maximum, and mean ADC values were recorded from intralesional ROIs as well as from ROIs placed in nearby muscle, and values across slices were averaged. The ADC ratio was defined as the ratio of the intralesional ADC value to the ADC value of muscle, similar to the methods previously described for normalizing ADC values [18].

Third, the subset of solid STMs with high fluid content (high T2 ratios, as above) was analyzed to determine whether the ADC values of soft tissue tumors with high fluid signal intensity on unenhanced sequences significantly differed from the ADC values of cysts.

Statistical analysis

First, descriptive statistics were reported. Differences in age and gender between subjects with cysts and those with solid masses were compared using Wilcoxon rank-sum and Fisher's exact test. Second, all continuous variables (T2 signal ratio, minimum, maximum, and mean lesion ADC value, lesion:muscle ADC ratio) were compared for cysts and solid STMs by Wilcoxon rank-sum using means derived from the two readers' measurements; inter-observer agreement was assessed using the intra-class correlation coefficient (ICC). Qualitative scores of DWI appearance were dichotomized to "low" or "high" signal loss and compared for cysts and solid STMs using Fisher's exact test. Third, ADC values recorded from the subset of solid soft tissue tumors with T2 hyperintensity mimicking fluid were compared with ADC values recorded from cysts (Wilcoxon). Fourth, ADC values recorded

from benign and malignant solid STMs were compared (Wilcoxon). Fifth, receiver-operating characteristic (ROCs) were constructed for T2 signal ratios, and minimum, maximum, and mean ADC values for differentiating solid and non-solid STMs for each observer; ROCs were also constructed for comparing solid STMs of high fluid signal intensity and true cysts. Differences were considered significant at $p < 0.05$. The statistical analysis was performed using Stata 11.1 (StataCorp, College Station, TX, USA).

Results

For the 36 subjects with 37 STMs, there were 10 cysts and 27 solid STMs (Table 1). There was no difference in the mean subject age for those with cysts and those with solid STMs (51.0 ± 29.6 vs 46.3 ± 17.4 years, $p = 0.22$, Wilcoxon). There was no difference in gender composition between the two groups (46 % [12 out of 26] female for solid STMs vs 40 % [4 out of 10] female for cysts, $p = 1.0$, Fisher's exact).

Table 2 shows the T2 signal ratios, DWI measures and ADC values of cysts and solid STMs in our population. There was a significant difference in both the T2 signal ratios and ADC values of cysts (Fig. 1) and solid STMs (Figs. 2, 3). Inter-reader variability was good for ADC minimum values (ICC=0.76), and was excellent for ADC maximum (ICC=0.87), ADC mean (ICC=0.93), and T2 signal ratio (ICC=0.95). In the qualitative assessment of signal on successive DWI sequences, 22 non-solid lesions showed low signal loss, and 5 scored as high signal loss; 4 non-solid lesions scored low signal loss, and 6 scored high ($p = 0.04$, Fisher's exact).

For all STMs, area under the ROC (AUC) for T2 ratio, minimum, maximum, and mean ADC were 0.71, 0.82, 0.76, and 0.81 respectively, for distinguishing cysts from solid STMs (Fig. 4a). Using threshold ADC values of 1.8 (minimum ADC) or 2.5 (mean ADC) yielded a sensitivity of 60 % and 80 % respectively, and a specificity of 100 % for classifying a STM as a cyst. These cut-off points yielded positive predictive values of 100 %, and negative predictive values of 87 % and 93 % respectively; using these thresholds resulted in overall accuracy of 89 % and 95 % in classifying lesions as cysts or solid STMs.

A subset of 9 solid STMs met the criteria for having high fluid-like signal intensity using a quantitative threshold T2 signal ratio of 2.8; this was the lowest T2 signal ratio for an uncomplicated cyst (i.e., non-hematoma or abscess). For this subset, the mean of the T2 signal ratios was actually higher for the group of solid masses compared with the true cysts, although this did not reach statistical significance (Table 2). Minimum and mean ADC measurements of these solid tumors with high fluid signal were significantly lower than for cysts. The threshold minimum ADC value of 1.3 yielded a sensitivity/specificity of 70 %/100 %; a mean ADC value of 2.5 yielded a sensitivity of 80 %, specificity of 100 %, and overall accuracy of 89 % for distinguishing solid STMs of high fluid content from cysts. High AUCs were maintained for maximum (AUC=0.71), minimum (AUC=0.81), and mean (AUC=0.80) ADC values in this subset of patients, but performance was substantially weaker for T2 signal ratio (AUC=0.37). Figure 2 highlights the utility of the ADC map for distinguishing a solid tumor (myxoid sarcoma) from adjacent fluid.

Of the 27 solid STMs, 12 were pathologically confirmed malignant tumors and 15 were pathologically confirmed benign lesions. Excluding all cysts, minimum and mean ADC values were significantly lower in malignant STMs compared with benign STMs (minimum ADC: 0.52 ± 0.39 vs 0.81 ± 0.29 respectively, $p=0.04$; mean ADC: 1.21 ± 0.36 vs 1.64 ± 0.27 respectively, $p=0.004$). Between malignant and benign solid STMs, there was no difference in the maximum ADC value (2.28 vs 2.34 respectively, $p=0.66$). Using a mean ADC of >1.7 yielded a sensitivity of 40 %, a specificity of 92 %, and an accuracy of 63 % in classifying lesions as benign.

Discussion

Quantitative DWI with ADC mapping is an accurate technique for separating non-neoplastic cysts from solid musculoskeletal STMs, and a valuable addition to a routine MRI protocol for the characterization of an STM. Importantly, DWI is an unenhanced method that is particularly useful in instances where intravenous contrast medium administration is precluded owing to renal failure, prior adverse reaction, or refused by the patient, and can be obtained with minimal additional imaging time (~ 2.5 min). However, it should be stressed that aside from distinguishing cysts from solid tumors, contrast medium administration, particularly when employing a dynamic technique, helps to assess treatment response, evaluate for post-operative recurrence and define tumor extent. DWI does not replace intravenous contrast for all these roles, but its usefulness as an adjunct sequence for these roles is an area of active investigation.

The results of this study are in agreement with previous studies of STMs evaluated by DWI, which have shown that areas of restricted diffusion reflect cellular tissue found in tumors [20, 21]. Therefore, interrogation of a non-cellular cyst by quantitative DWI is expected to show high ADC values. In our study, a threshold mean ADC value of 2.5 provided 100 % specificity for predicting a cyst and ruling out a solid tumor, even for T2 hyperintense solid masses, which can mimic cysts on unenhanced sequences. Such data suggest that quantitative DWI can supplement a conventional imaging protocol and perhaps replace the need for contrast-enhanced imaging for the specific purpose of distinguishing a cyst from a solid tumor when the ADC value is higher than 2.5. This value is in line with reports from the literature for mean ADC values in cysts in other tissues, such as the liver [22].

Among the non-solid STMs in this study were a hematoma (ADC minimum=0.56, maximum=1.53, and mean=0.82) and an abscess (ADC minimum=0.15, maximum=1.30, and mean=0.63) with ADC profiles different from other cysts. With regard to hematomas, these ADC values stand in contrast to recent results showing consistently higher ADC values in chronic soft tissue hematomas compared with malignant tumors [23]. Such a discrepancy between our case of a hematoma and the literature may be due to differences in the stages of hematoma evolution [24], as early stage intracranial hematomas (those biophysical states in which erythrocytes remain intact) are known to show low ADC values [25]; more work should be done to assess how ADC values correlate with varying ages of soft tissue hematomas. With regard to abscesses, our low ADC measurements agree with low ADC values that have been reported in soft tissue abscesses [26, 27]. Hence, the need for comprehensive sequence selection and the importance of clinical information

in assessing STMs is underscored by these cases, to avoid mischaracterization of a cyst as a solid mass based on ADC measurements alone. A protocol with intravenous contrast medium will still be needed in these instances, in particular when there is a high pre-test probability of infection or hematoma.

An important pitfall in the interpretation of STMs is mistaking solid soft tissue tumors with high fluid content, such as myxoid neoplasms and synovial sarcoma [28, 29], for cysts. In this study, peripheral nerve sheath tumors illustrated a similar phenomenon. The ratio of lesion:muscle T2-signal was used to quantify the degree of similarity between the T2 signal of such STMs and those of true cysts. Notably, in the subset of very T2 hyperintense soft tissue tumors in this population, the ADC threshold value of 2.5 was maintained and excluded the diagnosis of a cyst in all cases. As such, ADC measurements may be of great value for detecting a neoplasm when an STM appears “cystic.”

A secondary purpose of this study was the characterization of solid STMs. First, in this series, all solid STMs had histological confirmation rather than relying on contrast enhancement for diagnosis. Very infrequently, solid STMs will show no enhancement internally, mimicking a cyst. In such settings, ADC values may be critical in guiding the diagnosis toward a solid mass. Second, there is controversy regarding whether quantitative DWI can reliably discriminate between malignant neoplasms and benign solid STMs, as there is overlap in their ADC values. There are reports that have failed to show a significant difference in the ADC values between benign and malignant tumors [6, 8–10]. Our findings add support to the line of evidence that lower ADC values are associated with malignancy [11, 23, 30], even when benign cysts, which have a higher ADC, were removed from the analysis. These findings are also in keeping with the broader oncology literature showing that low ADC values are associated with malignancy in a variety of soft tissues throughout the body [31, 32]. One limitation of constructing ROIs within a STM is the potential for significant sampling error if care is not taken to include an adequately large region of interest in big or heterogeneous masses. However, in this study, differences in ROI construction between observers resulted in minimal differences in measured ADC values, as reflected by good to excellent ICC values. The ICC was lower for maximum and minimum ADC values than for T2 ratio and mean ADC values, likely because maximum and minimum values selectively bias toward extreme values, exaggerating differences between observers and hence lowering the ICC.

It has been recommended that at least three b-values be used for performing DWI with ADC quantification [5]. Our protocol used b-values of 50, 400, and 800 s/mm² for the calculation of the ADC map. While there is empirical evidence indicating that additional b-values might not increase the precision of ADC calculations [33], selection of b-values is critically important, as use of higher b-values will preferentially sample the more slowly diffusing tissue pools, leading to lower ADC values [34]. Higher b-values also suffer degradations in signal-to-noise ratio. Optimal selection of b-values has not yet been rigorously defined for musculoskeletal soft tissues, but our selection is within the range of values recommended in prior reports [6]. Other DWI studies have utilized only two b-values, potentially another reason for conflicting results in ADC measurements of musculoskeletal lesions in the literature.

This study has several limitations. First, histological confirmation was not available for all cysts, as most cysts were determined by the absence of internal contrast enhancement, their characteristic location and clinical presentation with at least a 3-month follow-up confirming the diagnosis. Diagnostic and therapeutic parsimony dictates that histological confirmation of such characteristically benign cysts will rarely be available in any series. Second, our sample size of 35 cases is relatively small, but similar to that of other studies that examined the utility of DWI in musculoskeletal soft tissue lesions [8, 11, 23]. Third, the potential for selection bias is recognized, as cases were initially identified through the PACS system by an observer who had prospectively interpreted approximately one third of the cases. Fourth, ADC maps used in this study were based on a monoexponential fit of signal decay with increasing b-values; theoretically, utilizing a multiexponential fit would be more appropriate for biological tissues. Biexponential fitting of multi-b-value DWI has been shown to provide better accuracy compared with ADC values obtained with a monoexponential fit in discriminating enhancing from non-enhancing renal lesions [35], but this comes at the cost of increased imaging time required for the acquisition of multiple b-values.

It should be emphasized that ultrasound plays an important role in the evaluation of soft tissue masses and is accurate in determining whether a lesion is solid or cystic; however, MRI offers the best single imaging modality for simultaneously assessing the locoregional extent of the disease, relation of tumor with compartmental anatomy, cortical or intraosseous involvement, extent of tumor necrosis, and involvement of the neurovascular bundle [36]. Even when a cystic lesion is diagnosed at ultrasound, its benignity cannot be guaranteed unless it is found in a characteristic location or relation to a synovial joint to allow diagnosis of a Baker's cyst or ganglion [37, 38]. Low rates of interobserver agreement in diagnostic ultrasound for soft tissue masses [39], coupled with the reasons listed above, have made MRI the preferred imaging modality for the initial assessment of soft tissue masses at our institution. It should also be noted that small solid masses or nodular components of larger cystic masses that are below approximately 1 cm in size may be inaccurately characterized on DWI because of limitations in spatial resolution—careful attention to subtle areas of heterogeneity in T2 signal and irregularities in cyst wall contours on higher resolution sequences are required so that one does not overlook neoplasm.

In conclusion, it is unlikely that a single sequence, such as DWI, will routinely provide a definitive method for the characterization of all STMs. An optimal approach to STM characterization will include information derived from all available MR sequences. However, this study shows that quantitative DWI with ADC values >2.5 can provide high specificity for the purpose of distinguishing cysts and solid tumors. Future investigations should include a wide group of non-solid and solid lesions, including recruitment of subjects with abscesses and hematomas of different stages, to more comprehensively assess the performance of quantitative DWI in identifying such lesions.

Conflicts of interest

The authors wish to disclose the following conflicts of interest: grant support from GE Radiology Research Academic Fellowship and Siemens Healthcare.

References

1. Gielen JLMA, De Schepper AM, Vanhoenacker F, Parizel PM, Wang XL, Sciort R, et al. Accuracy of MRI in characterization of soft tissue tumors and tumor-like lesions. A prospective study in 548 patients. *Eur Radiol.* 2004;14(12):2320–30. [PubMed: 15290067]
2. Wu JS, Hochman MG. Soft-tissue tumors and tumorlike lesions: a systematic imaging approach. *Radiology.* 2009;253(2):297–316. [PubMed: 19864525]
3. Frassica FJ, Khanna JA, McCarthy EF. The role of MR imaging in soft tissue tumor evaluation: perspective of the orthopedic oncologist and musculoskeletal pathologist. *Magn Reson Imaging Clin N Am.* 2000;8(4):915–27. [PubMed: 11149686]
4. Le Bihan D, Breton E, Lallemand D, Grenier P, Cabanis E, Laval-Jeantet M. MR imaging of intravoxel incoherent motions: application to diffusion and perfusion in neurologic disorders. *Radiology.* 1986;161(2):401–7. [PubMed: 3763909]
5. Padhani AR, Liu G, Koh DM, Chenevert TL, Thoeny HC, Takahara T, et al. Diffusion-weighted magnetic resonance imaging as a cancer biomarker: consensus and recommendations. *Neoplasia.* 2009;11(2):102–25. [PubMed: 19186405]
6. Khoo MMY, Tyler PA, Saifuddin A, Padhani AR. Diffusion-weighted imaging (DWI) in musculoskeletal MRI: a critical review. *Skeletal Radiol.* 2011;40(6):665–81. [PubMed: 21311884]
7. Costa FM, Ferreira EC, Vianna EM. Diffusion-weighted magnetic resonance imaging for the evaluation of musculoskeletal tumors. *Magn Reson Imaging Clin N Am.* 2011;19(1):159–80. [PubMed: 21129640]
8. Einarsdóttir H, Karlsson M, Wejde J, Bauer HCF. Diffusion-weighted MRI of soft tissue tumours. *Eur Radiol.* 2004;14(6):959–63. [PubMed: 14767604]
9. Maeda M, Matsumine A, Kato H, Kusuzaki K, Maier SE, Uchida A, et al. Soft-tissue tumors evaluated by line-scan diffusion-weighted imaging: influence of myxoid matrix on the apparent diffusion coefficient. *J Magn Reson Imaging.* 2007;25(6):1199–204. [PubMed: 17520732]
10. Nagata S, Nishimura H, Uchida M, Sakoda J, Tonan T, Hiraoka K, et al. Diffusion-weighted imaging of soft tissue tumors: usefulness of the apparent diffusion coefficient for differential diagnosis. *Radiat Med.* 2008;26(5):287–95. [PubMed: 18661213]
11. Van Rijswijk CSP, Kunz P, Hogendoorn PCW, Taminiau AHM, Doornbos J, Bloem JL. Diffusion-weighted MRI in the characterization of soft-tissue tumors. *J Magn Reson Imaging.* 2002;15(3):302–7. [PubMed: 11891975]
12. Jin G, An N, Jacobs MA, Li K. The role of parallel diffusion-weighted imaging and apparent diffusion coefficient (ADC) map values for evaluating breast lesions: preliminary results. *Acad Radiol.* 2010;17(4):456–63. [PubMed: 20207316]
13. Teo EL, Strouse PJ, Hernandez RJ. MR imaging differentiation of soft-tissue hemangiomas from malignant soft-tissue masses. *AJR Am J Roentgenol.* 2000;174(6):1623–8. [PubMed: 10845496]
14. Moteki T, Horikoshi H, Endo K. Relationship between apparent diffusion coefficient and signal intensity in endometrial and other pelvic cysts. *Magn Reson Imaging.* 2002;20(6):463–70. [PubMed: 12361793]
15. Jacobs MA, Ouwerkerk R, Kamel I, Bottomley PA, Bluemke DA, Kim HS. Proton, diffusion-weighted imaging, and sodium (^{23}Na) MRI of uterine leiomyomata after MR-guided high-intensity focused ultrasound: a preliminary study. *J Magn Reson Imaging.* 2009;29(3):649–56. [PubMed: 19243047]
16. Ogura A, Hayakawa K, Miyati T, Maeda F, Miyai A, Saeki F, et al. Differentiation of hepatic tumors by use of image contrast with T2-weighted MRI. *Radiol Phys Technol.* 2009;2(1):54–7. [PubMed: 20821129]
17. Ballesio L, Savelli S, Angeletti M, Porfiri LM, D'Ambrosio I, Maggi C, et al. Breast MRI: Are T2 IR sequences useful in the evaluation of breast lesions? *Eur J Radiol.* 2009;71(1):96–101. [PubMed: 18479866]
18. Ei Khouli RH, Jacobs MA, Mezban SD, Huang P, Kamel IR, Macura KJ, et al. Diffusion-weighted imaging improves the diagnostic accuracy of conventional 3.0-T breast MR imaging. *Radiology.* 2010;256(1):64–73. [PubMed: 20574085]

19. Aprile I, Iaiza F, Lavaroni A, Budai R, Dolso P, Scott CA, et al. Analysis of cystic intracranial lesions performed with fluid-attenuated inversion recovery MR imaging. *AJNR Am J Neuroradiol.* 1999;20(7):1259–67. [PubMed: 10472983]
20. Baur A, Huber A, Arbogast S, Dürr HR, Zysk S, Wendtner C, et al. Diffusion-weighted imaging of tumor recurrences and posttherapeutical soft-tissue changes in humans. *Eur Radiol.* 2001;11(5):828–33. [PubMed: 11372617]
21. Sugahara T, Korogi Y, Kochi M, Ikushima I, Shigematu Y, Hirai T, et al. Usefulness of diffusion-weighted MRI with echo-planar technique in the evaluation of cellularity in gliomas. *J Magn Reson Imaging.* 1999;9(1):53–60. [PubMed: 10030650]
22. Taouli B, Koh D-M. Diffusion-weighted MR imaging of the liver. *Radiology.* 2010;254(1):47–66. [PubMed: 20032142]
23. Oka K, Yakushiji T, Sato H, Yorimitsu S, Hayashida Y, Yamashita Y, et al. Ability of diffusion-weighted imaging for the differential diagnosis between chronic expanding hematomas and malignant soft tissue tumors. *J Magn Reson Imaging.* 2008;28(5):1195–200. [PubMed: 18972359]
24. Siegel MJ. Magnetic resonance imaging of musculoskeletal soft tissue masses. *Radiol Clin N Am.* 2001;39(4):701–20. [PubMed: 11549166]
25. Atlas SW, DuBois P, Singer MB, Lu D. Diffusion measurements in intracranial hematomas: implications for MR imaging of acute stroke. *AJNR Am J Neuroradiol.* 2000;21(7):1190–4. [PubMed: 10954267]
26. Unal O, Koparan HI, Avcu S, Kalender AM, Kisli E. The diagnostic value of diffusion-weighted magnetic resonance imaging in soft tissue abscesses. *Eur J Radiol.* 2011;77(3):490–4. [PubMed: 19748752]
27. Harish S, Chiavaras MM, Kotnis N, Rebello R. MR imaging of skeletal soft tissue infection: utility of diffusion-weighted imaging in detecting abscess formation. *Skeletal Radiol.* 2011;40(3):285–94. [PubMed: 20552358]
28. Kransdorf MJ, Jelinek JS, Moser RP Jr, Utz JA, Brower AC, Hudson TM, et al. Soft-tissue masses: diagnosis using MR imaging. *AJR Am J Roentgenol.* 1989;153(3):541–7. [PubMed: 2763953]
29. Murphey MD, Gibson MS, Jennings BT, Crespo-Rodríguez AM, Fanburg-Smith J, Gajewski DA. From the archives of the AFIP: Imaging of synovial sarcoma with radiologic-pathologic correlation. *Radiographics.* 2006;26(5):1543–65. [PubMed: 16973781]
30. Razek A, Nada N, Ghaniem M, Elkhamary S. Assessment of soft tissue tumours of the extremities with diffusion echoplanar MR imaging. *Radiol Med.* 2012;117(1):96–101. [PubMed: 21744251]
31. Koh D-M, Collins DJ. Diffusion-weighted MRI in the body: applications and challenges in oncology. *AJR Am J Roentgenol.* 2007;188(6):1622–35. [PubMed: 17515386]
32. Malayeri AA, El Khoul RH, Zaheer A, Jacobs MA, Corona-Villalobos CP, Kamel IR, et al. Principles and applications of diffusion-weighted imaging in cancer detection, staging, and treatment follow-up. *Radiographics.* 2011;31(6):1773–91. [PubMed: 21997994]
33. Bogner W, Gruber S, Pinker K, Grabner G, Stadlbauer A, Weber M, et al. Diffusion-weighted MR for differentiation of breast lesions at 3.0 T: how does selection of diffusion protocols affect diagnosis? *Radiology.* 2009;253(2):341–51. [PubMed: 19703869]
34. Clark CA, Le Bihan D. Water diffusion compartmentation and anisotropy at high b values in the human brain. *Magn Reson Med.* 2000;44(6):852–9. [PubMed: 11108621]
35. Chandarana H, Lee VS, Hecht E, Taouli B, Sigmund EE. Comparison of biexponential and monoexponential model of diffusion weighted imaging in evaluation of renal lesions: preliminary experience. *Invest Radiol.* 2011;46(5):285–91. [PubMed: 21102345]
36. De Schepper AM, De Beuckeleer L, Vandevenne J, Somville J. Magnetic resonance imaging of soft tissue tumors. *Eur Radiol.* 2000;10(2):213–23. [PubMed: 10663750]
37. Jacobson JA. Musculoskeletal ultrasound and MRI: which do I choose? *Semin Musculoskelet Radiol.* 2005;9(2):135–49. [PubMed: 16044382]
38. Ward EE, Jacobson JA, Fessell DP, Hayes CW, van Holsbeeck M. Sonographic detection of Baker's cysts: comparison with MR imaging. *AJR Am J Roentgenol.* 2001;176(2):373–80. [PubMed: 11159077]
39. Wu S, Tu R, Liu G, Shi Y. Role of ultrasound in the diagnosis of common soft tissue lesions of the limbs. *Ultrasound Q.* 2013;29(1):67–71. [PubMed: 23370782]

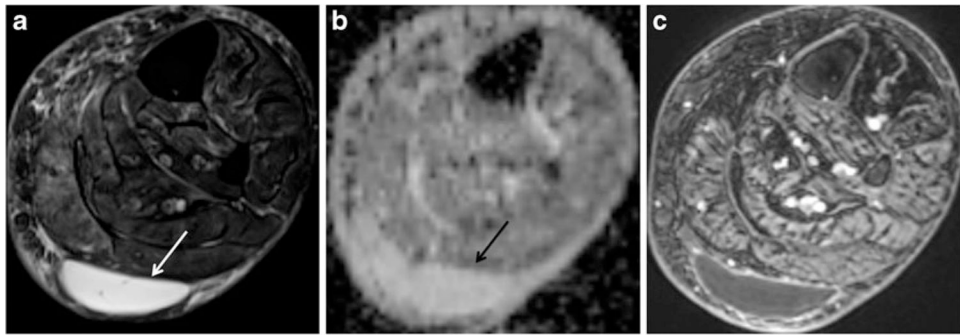


Fig. 1.

A 59-year-old woman with a posterior calf mass that resolved with follow-up. **a** Axial T2-weighted image with fat suppression (FSE, TR/TE 4,060/71 ms) shows a well-defined hyperintense mass (*arrow*) in the superficial soft tissues of the calf posterior to the gastrocnemius muscles. **b** Axial ADC map reveals the mass to have high ADC values (mean ADC value of 2.82). **c** Post-contrast image (VIBE, TR/TE 6.35/1.48) clearly shows the non-enhancing soft tissue mass (STM) as a cyst

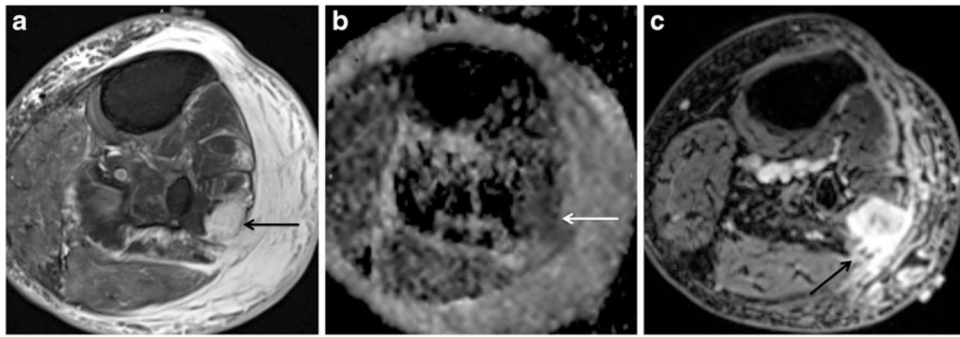


Fig. 2.

An 87-year-old woman with a calf mass. **a** Axial T2-weighted image with fat suppression (FSE, TR/TE 4,060/71 ms) shows an ill-defined hyperintense mass (*arrow*) involving the peroneal muscles, very similar in signal intensity to adjacent subcutaneous fluid (T2 ratio of 2.6). The surrounding soft tissue edema blurs the margins of the mass and complicates the assessment of extent. **b** Axial ADC map reveals a region of low ADC values (*white arrow*) in the area corresponding to the tumor (mean ADC value of 1.69). **c** Post-contrast image (VIBE, TR/TE 6.35/1.48) clearly shows the enhancing STM separate from the subcutaneous tissues (*arrow*). Biopsy revealed an intermediate grade myxoid sarcoma

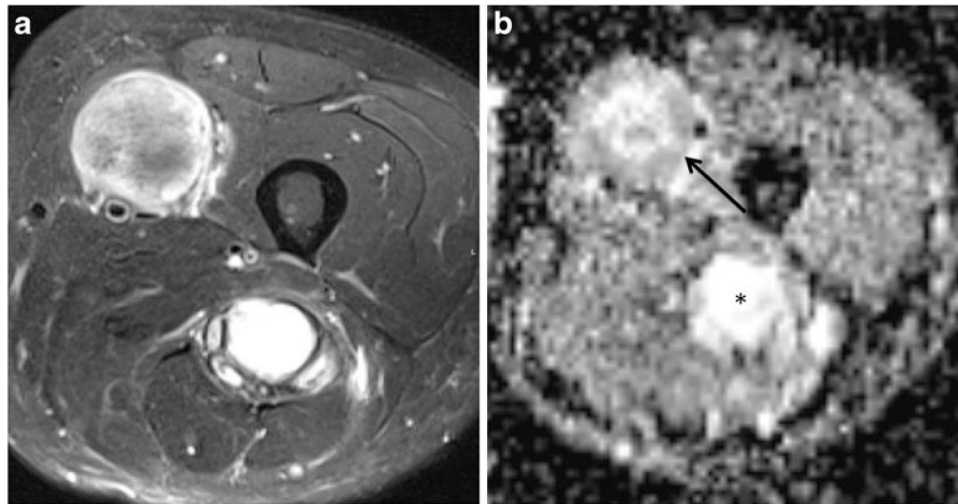


Fig. 3.

A 53-year-old man with neurofibromatosis type 1 with two STMs in the thigh. **a** Axial T2-weighted image with fat suppression (FSE, TR/TE 4,060/71 ms) shows two masses, the first associated with the femoral nerve in the anterior thigh of variable signal, and the second associated with the sciatic nerve in the posterior thigh of high signal. The T2 signal ratios for these lesions were 2.05 and 4.38 respectively. **b** Axial ADC map shows mean ADC value of 1.37 in the anterior mass (*arrow*) and 2.04 (*asterisk*) in the posterior thigh mass. Biopsy of these STMs revealed a malignant peripheral nerve sheath tumor in the anterior thigh and a localized neurofibroma in the posterior thigh. This case highlights the potential role for quantitative DWI in distinguishing benign (posterior mass) and malignant (anterior mass) tumors

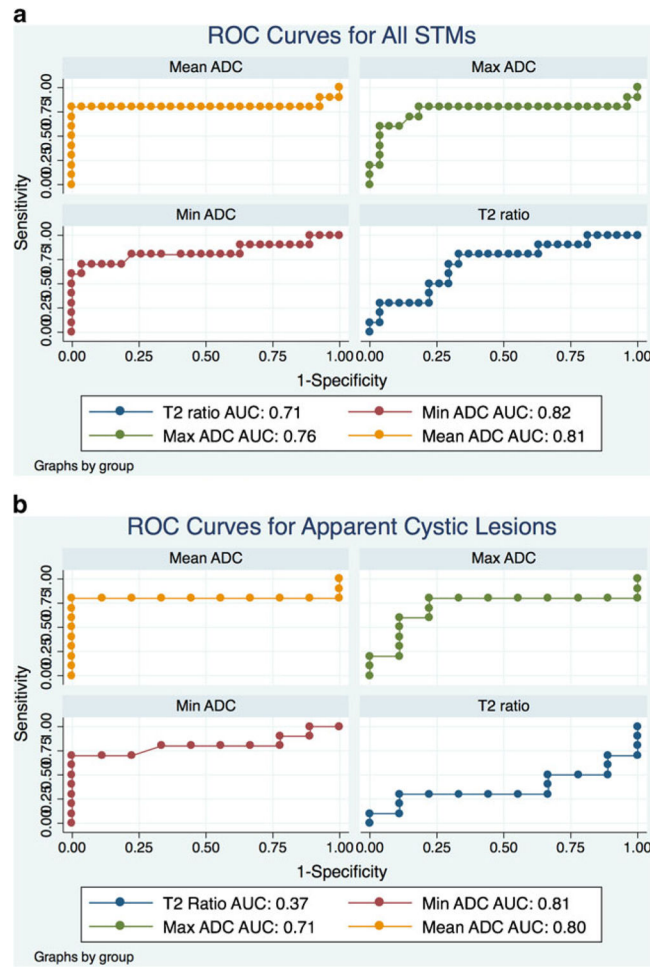


Fig. 4. **a** Receiver operating characteristic (ROC) analysis of T2 signal ratio (lesion:muscle), minimum ADC, maximum ADC, mean ADC, and the mean ADC ratio (lesion:muscle) for distinguishing between non-solid and solid STMs. Performance for each variable is given by area under the curve (AUC); better performance is indicated by high AUC. ADC values performed well, but performance was not statistically superior to the quantitative T2 signal ratio ($p=0.23$). **b** In the subset of cystic-appearing solid STMs, mean, maximum, and minimum ADC all demonstrated significantly better performance ($p=0.003$, 0.03 and <0.001 respectively) than the quantitative T2 signal ratio

Table 1

Summary of demographic and individual soft tissue mass (STM) characteristics

| ID | Sex | Age (years) | Diagnosis | Classification: solid/cystic | Contrast enhancement pattern | Additional diagnostic criteria | T2 | Minimum ADC | Maximum ADC | Mean ADC | Ratiomusc ADC |
|----|--------|-------------|--------------------------------|------------------------------|------------------------------|--------------------------------|-------|-------------|-------------|----------|---------------|
| 1 | Female | 82 | Paralabral cyst | Non-solid | None | Clinical follow-up | 5.65 | 2.35 | 2.99 | 2.68 | 2.37 |
| 2 | Male | 78 | Ganglion | Non-solid | None | Clinical follow-up | 3.98 | 1.82 | 2.75 | 2.52 | 1.64 |
| 3 | Male | 59 | Prepatellar bursitis | Non-solid | None | Histological | 4.08 | 2.43 | 4.10 | 3.17 | 2.26 |
| 4 | Male | 4 | Lymphatic malformation | Non-solid | None | Clinical follow-up | 3.45 | 1.00 | 2.97 | 2.56 | 2.20 |
| 5 | Male | 64 | Hematoma | Non-solid | None | Clinical follow-up | 2.22 | 0.56 | 1.53 | 0.82 | 0.56 |
| 6 | Male | 4 | Baker's cyst | Non-solid | None | Clinical follow-up | 14.64 | 2.01 | 3.17 | 2.64 | 7.13 |
| 7 | Female | 59 | Seroma | Non-solid | None | Clinical follow-up | 5.32 | 2.62 | 3.14 | 2.82 | 1.61 |
| 8 | Female | 22 | Abscess | Non-solid | N/A | Histological | 1.48 | 0.15 | 1.30 | 0.63 | 1.58 |
| 9 | Female | 75 | Ganglion | Non-solid | None | Histological | 3.48 | 1.30 | 3.40 | 2.63 | 1.95 |
| 10 | Male | 63 | Ganglion | Non-solid | None | Clinical follow-up | 2.80 | 2.25 | 2.80 | 2.59 | 1.90 |
| 11 | Male | 33 | Metastasis (squamous cell) | Solid | Nodular | Histological | 2.50 | 1.13 | 2.31 | 1.84 | 1.55 |
| 12 | Female | 47 | PNST | Solid | Nodular | Histological | 2.03 | 0.90 | 2.92 | 1.95 | 4.06 |
| 13 | Female | 38 | PNST | Solid | Heterogeneous | Histological | 2.50 | 0.68 | 2.80 | 1.53 | 15.21 |
| 14 | Female | 51 | Fibroblastic proliferation | Solid | Nodular | Histological | 1.35 | 0.96 | 1.58 | 1.32 | 0.98 |
| 15 | Male | 63 | Metastasis (melanoma) | Solid | Homogeneous | Histological | 1.37 | 0.71 | 1.96 | 1.15 | 0.74 |
| 16 | Male | 61 | Fibrosarcoma | Solid | Heterogeneous | Histological | 1.03 | 0.10 | 2.14 | 0.78 | 1.83 |
| 17 | Female | 22 | Desmoid | Solid | Homogeneous | Histological | 2.51 | 0.29 | 2.00 | 1.38 | 1.17 |
| 18 | Male | 52 | Metastasis (papillary thyroid) | Solid | Homogeneous | Histological | 1.98 | 0.38 | 1.51 | 0.90 | 0.83 |
| 19 | Male | 56 | MPNST | Solid | Heterogeneous | Histological | 2.31 | 0.50 | 2.24 | 0.89 | 2.11 |
| 20 | Male | 61 | Fibroadipose tissue | Solid | Nodular | Histological | 2.63 | 0.75 | 2.28 | 1.47 | 1.58 |
| 21 | Male | 45 | PNST | Solid | Nodular | Histological | 1.67 | 0.13 | 2.37 | 1.56 | 1.10 |
| 22 | Female | 19 | MPNST | Solid | Heterogeneous/ Nodular | Histological | 3.89 | 0.00 | 3.32 | 1.62 | 2.60 |
| 23 | Male | 40 | Exuberant inflammation | Solid | Heterogeneous | Histological | 1.54 | 1.11 | 1.86 | 1.49 | 1.09 |
| 24 | Male | 25 | Ganglioneuroma (path) | Solid | Heterogeneous | Histological | 4.69 | 0.72 | 2.72 | 1.74 | 1.86 |

| ID | Sex | Age (years) | Diagnosis | Classification: solid/cystic | Contrast enhancement pattern | Additional diagnostic criteria | T2 | Minimum ADC | Maximum ADC | Mean ADC | Ratiosusc |
|----|--------|-------------|--------------------------------------|------------------------------|------------------------------|--------------------------------|------|-------------|-------------|----------|-----------|
| 25 | Male | 65 | Pleomorphic undifferentiated sarcoma | Solid | Heterogeneous | Histological | 3.17 | 0.31 | 2.01 | 1.03 | 0.84 |
| 26 | Male | 27 | Inflammatory fibrovascular tissue | Solid | Homogeneous | Histological | 1.32 | 0.66 | 2.03 | 1.45 | 1.08 |
| 27 | Female | 57 | Ewing's sarcoma (extraosseous) | Solid | Heterogeneous | Histological | 2.68 | 0.19 | 2.79 | 0.80 | 0.48 |
| 28 | Female | 87 | Myxoid sarcoma | Solid | Heterogeneous | Histological | 2.64 | 1.31 | 2.20 | 1.69 | 0.97 |
| 29 | Female | 34 | MPNST | Solid | Heterogeneous | Histological | 4.31 | 0.67 | 2.41 | 1.32 | 1.43 |
| 30 | Female | 39 | PVNS | Solid | Homogeneous | Histological | 0.83 | 0.97 | 1.99 | 1.46 | 0.91 |
| 31 | Male | 53 | MPNST | Solid | Heterogeneous | Histological | 2.05 | 0.55 | 2.47 | 1.37 | 1.33 |
| 32 | Male | 53 | PNST | Solid | Heterogeneous | Histological | 4.38 | 0.94 | 2.70 | 2.04 | 1.89 |
| 33 | Female | 55 | PNST | Solid | Heterogeneous | Histological | 3.65 | 0.90 | 2.65 | 1.95 | 1.18 |
| 34 | Female | 73 | PNST | Solid | Homogeneous | Histological | 5.16 | 1.00 | 1.85 | 1.40 | 1.08 |
| 35 | Female | 17 | MPNST | Solid | Heterogeneous | Histological | 2.52 | 0.35 | 2.00 | 1.10 | 0.92 |
| 36 | Male | 53 | PNST | Solid | Homogeneous | Histological | 5.14 | 1.05 | 2.50 | 1.72 | 1.81 |
| 37 | Male | 25 | PNST | Solid | Heterogeneous | Histological | 9.82 | 1.15 | 2.85 | 2.15 | 1.43 |

In addition to contrast enhancement pattern suggesting non-solid or solid nature, report of any confirmatory diagnostic information is given in this column, regarding available histology or clinical follow-up

ADC=apparent diffusion coefficient, reported in $10^{-3} \text{ mm}^2/\text{s}$; T2 = T2 lesion/T2 muscle signal ratio; ratiosusc = mean ADC lesion/mean ADC muscle ratio; PNST=peripheral nerve sheath tumor;

MPNST=malignant peripheral nerve sheath tumor; PVNS=pigmented villonodular synovitis

Table 2

Summary of T2 signal ratios and ADC values in solid and non-solid STMs

| | T2 signal ratio | Minimum ADC | Maximum ADC | Mean ADC | Lesion:muscle Mean ADC ratio |
|--|-----------------|-------------|-------------|-----------|------------------------------|
| Solid (<i>n</i> =27) | 2.94±1.85 | 0.68±0.37 | 2.31±0.43 | 1.45±0.38 | 1.93±2.75 |
| Non-solid (<i>n</i> = 10) | 4.71±3.72 | 1.65±0.85 | 2.81±0.83 | 2.31±0.85 | 2.32±1.77 |
| <i>p</i> value | 0.05 | 0.003 | 0.02 | 0.005 | 0.02 |
| AUC | 0.71 | 0.82 | 0.76 | 0.81 | 0.75 |
| Cystic-appearing solid STMs (<i>n</i> =9) | 4.91±1.95 | 0.75±0.38 | 2.56±0.44 | 1.66±0.36 | 1.57±0.53 |
| <i>p</i> value vs non-solid lesions | 0.32 | 0.02 | 0.12 | 0.03 | 0.12 |
| AUC | 0.37 | 0.81 | 0.71 | 0.80 | 0.71 |

The first comparison is between solid and non-solid soft tissue masses. The second comparison between cystic appearing STMs and non-solid lesions shows that solid lesions that appear similar to cysts on T2-weighted images can be better distinguished from non-solid lesions by ADC values. Values given are mean±standard deviation

ADC=apparent diffusion coefficient, reported in $10^{-3} \text{ mm}^2/\text{s}$; AUC=area under the receiver operating characteristic